

Citation for published version:

Welch, M, Cook, K, Correa, RA, Gerome, F, Wadsworth, W, Gorbach, A, Skryabin, D & Knight, J 2009, 'Solitons in hollow core photonic crystal fiber: Engineering nonlinearity and compressing pulses', *Journal of Lightwave Technology*, vol. 27, no. 11, pp. 1644-1652. <https://doi.org/10.1109/JLT.2009.2019731>

DOI:

[10.1109/JLT.2009.2019731](https://doi.org/10.1109/JLT.2009.2019731)

Publication date:

2009

Document Version

Peer reviewed version

[Link to publication](#)

© 2009 IEEE. Personal use of this material is permitted. Permission from IEEE must be obtained for all other uses, in any current or future media, including reprinting/republishing this material for advertising or promotional purposes, creating new collective works, for resale or redistribution to servers or lists, or reuse of any copyrighted component of this work in other works.

University of Bath

Alternative formats

If you require this document in an alternative format, please contact:
openaccess@bath.ac.uk

General rights

Copyright and moral rights for the publications made accessible in the public portal are retained by the authors and/or other copyright owners and it is a condition of accessing publications that users recognise and abide by the legal requirements associated with these rights.

Take down policy

If you believe that this document breaches copyright please contact us providing details, and we will remove access to the work immediately and investigate your claim.

Solitons in Hollow Core Photonic Crystal Fiber: Engineering Nonlinearity and Compressing Pulses

Matthew G. Welch, Kevin Cook, Rodrigo Amezcua Correa, Frédéric G  r  me, William J. Wadsworth, Andrey V. Gorbach, Dmitry V. Skryabin and Jonathan C. Knight.

Abstract— We have demonstrated nonlinear propagation in a 3-cell hollow core photonic crystal fiber. The reduced core size increases the nonlinear coefficient of the guided mode. However, the reduction in the expected soliton energy is small (a factor of approximately 2) as the dispersion of this fiber is also increased by the smaller core. We also demonstrate soliton compression using a 35m 7-cell tapered fiber, compressing picosecond input pulses by over an order of magnitude.

Index Terms—Optical fibers, Optical solitons, Optical propagation in nonlinear media, Optical pulse compression.

I. INTRODUCTION

Hollow core photonic crystal fiber (HC-PCF) is an ideal medium for the delivery of ultra-short, high peak power pulses. As the guidance mechanism of a photonic bandgap allows the use of an air core, the guided mode experiences low nonlinearity compared to conventional solid core fiber. The air core also means material dispersion is largely irrelevant. The dispersion is set by the waveguide dispersion of the defect that forms the core, and by the bandgap dispersion of the cladding. Therefore, scaling the cladding size (and simultaneously the core size) allows the dispersion curve to be shifted to different wavelengths.

These two facts make the delivery and manipulation of femtosecond solitons in HC-PCF viable over a wide range of wavelengths. Soliton delivery in HC-PCF was first demonstrated at 1.5  m wavelength by Ouzounov *et al* [1], and later by Luan *et al* at 800nm [2]. The ability of HC-PCF to deliver ultra-short pulses with several orders of magnitude higher peak power than conventional solid core fiber was revolutionary.

In this paper, we will first explore the nonlinear response of HC-PCF then discuss its use for soliton propagation and compression. We report two experimental studies; one of the nonlinear response of a 3-cell HC-PCF, and the second of

compression of picosecond pulses by a factor of more than 10 times using a 7-cell tapered HC-PCF.

II. PRINCIPLES

A. Nonlinearity

Nonlinearity in optical fibers causes a host of effects; self phase modulation (SPM), four-wave mixing and Raman gain to mention a few. For many applications, the delivery of ultra-short pulses using fiber optics at the highest possible pulse energies is desirable. However, if nonlinear effects dominate then the pulses' temporal and spectral shape will change radically during propagation.

As the (Kerr) nonlinear response of air is of the order of a thousand times less than that of silica, the maximum peak power that can be transmitted without nonlinear effects for a given pulse length is greatly increased in HC-PCF compared with a conventional solid core fiber. When combined with the unusual group-velocity dispersion of HC-PCF, which is anomalous over much of the low-loss transmission window, this makes HC-PCFs an obvious means to deliver high-power ultra-short pulses as optical solitons.

Optical solitons occur when the competing effects of anomalous dispersion and SPM counteract each other in exactly such a way that the pulse propagates as if affected by neither [3]. In a Raman inactive, loss-less medium, and in the absence of higher-order dispersion, the soliton existence condition is (1), [4].

$$\tau_{FWHM} = 1.76 \frac{N^2 \lambda^3 D A_{eff}}{2\pi^2 c n_2 E} \quad (1)$$

In (1), τ_{FWHM} is the temporal pulse length, N is the soliton order number ($N = 1$ for fundamental solitons), λ is the wavelength, D is the dispersion, A_{eff} is the effective area, n_2 is the Kerr nonlinear coefficient related to the third order nonlinear susceptibility tensor and E is the pulse energy.

Manuscript received November 12, 2008.

The Centre for Photonics and Photonic Materials and the Department of Physics, University of Bath, Bath, BA2 7AY UK. (e-mail: M.G.Welch@Bath.ac.uk). K. Cook is now at the Interdisciplinary Photonics Laboratories, University of Sydney. F. G  r  me is now at XLIM, University of Limoges.

The creation of solitons in HC-PCF previously required large and expensive amplified solid state laser systems, due to the high peak power requirements [1], [2]. However, recently it has been shown that an amplified mode-locked fiber laser has sufficient peak power to create picosecond and femtosecond solitons in such fibers. In fact, the use of the anomalous dispersion of the HC-PCF is a useful means of compensating the chirp that the output pulses from such a laser system acquires as a result of propagating through the amplifying fiber [5], [6], [7].

The energies available from femtosecond fiber lasers are of the order of the soliton energy in HC-PCF. Amplified solid state laser systems which provide an order of magnitude more energy are often used, but they are more expensive, require frequent servicing and have a large footprint. These factors rule out their use for many commercial and industrial applications. Therefore, if the nonlinearity of HC-PCF could be altered it would make them a more versatile choice for experiments with both amplified mode-locked fiber lasers and unamplified mode-locked bulk lasers. A HC-PCF with increased nonlinear response would help fill the gap (of several orders of magnitude!) in nonlinearity between large core silica fibers and regular HC-PCF, thus allowing the transmission of solitons with intermediate pulse energies.

The nonlinear response of a HC-PCF does not come solely from the air core. Part of the guided mode (typically ~1%) overlaps with the glass, and this contributes significantly to the Kerr nonlinearity because the nonlinear refractive index n_2 [4] of silica is three orders of magnitude greater than that of air. The approach we chose to increase the nonlinearity of HC-PCF was to fabricate a fiber in which the core consisted of a defect of 3 unit cells of the periodic cladding instead of the more common 7. Reducing the core area will not only increase the intensity of the light contained within the core but it will also increase the modal overlap with the silica cladding. A 3-cell fiber was previously reported by Petrovich *et al* [8].

It is worth noting that different 7-cell fibers (*i.e.* those with a core size of seven unit cells) can vary substantially in their optical response. Most 7-cell fibers are designed to have a mode that has very little overlap with the glass and a large transmission bandwidth. In order to achieve this, these fibers usually have a cladding with a very high air filling fraction (around 95%) and where the wall of glass surrounding the core has an optimized thickness [9], [10].

We modeled changing the pitch and air filling fraction of a 7-cell HC-PCF in such a way that the high frequency edge of the bandgap was fixed. We then calculated the effect that this has on both the dispersion and the nonlinearity as a function of wavelength, Fig. 1.

Increasing the air filling fraction and pitch in such a way, increases the spectral width of the bandgap. The increase in pitch also increases the core size reducing waveguide dispersion. These effects reduce the guided mode's overlap with the silica, reducing the Kerr nonlinear response (Fig. 1b). In a fiber the Kerr nonlinear response is often characterized using the nonlinear coefficient γ which in this paper is defined as (2) [4].

$$\gamma(\omega_0) = \frac{n_2(\omega_0) k_0}{A_{eff}} \quad (2)$$

where n_2 and A_{eff} are calculated using the method described in [11], and k_0 is the free space wavevector.

Changing the pitch from 5.5 μ m to 3.5 μ m (whilst keeping the high-frequency edge of the bandgap fixed) can increase the nonlinearity by as much as 4 times. However, this change in pitch also increases the dispersion by changing the dispersion slope. For example, 10nm away from the zero dispersion wavelength (ZDW) the dispersion is increased by a factor of 4. Hence, at this wavelength there would be no change in the soliton energy.

Therefore control of not only the nonlinearity but also of the dispersion is necessary for the creation of low energy solitons. A major cause of increased dispersion in HC-PCF is the core mode coupling to surface modes. As these surface modes are strongly peaked in the glass they are dispersive: they anti-cross with the core mode and strongly increase its dispersion. Surface modes can be thought of as arising due to an "imperfect termination" of the cladding around the core, and to reduce their impact, care has to be taken in choosing core geometries. For clarity the core wall thickness of the modeled fibers in Fig. 1 was chosen such that the effects of surface modes were reduced across much of the bandgap [9], [10].

B. Soliton Compression

There are two techniques for compressing a soliton in a waveguide; adiabatic compression and soliton effect compression. In soliton effect compression a higher-order soliton is initiated in the waveguide. In the absence of Raman scattering and higher-order dispersion (e.g. dispersion slope), higher-order solitons oscillate between a shorter, spectrally broader pulse and a narrower, but longer pulse, with the oscillation taking place over a distance called the soliton length [4]

$$Z_0 = \frac{\pi \tau_{FWHM}^2 c}{D \lambda^2} \quad (3).$$

Therefore, it is possible to compress a pulse simply by launching it as a higher-order soliton and ensuring that the pulse exits the fiber at the right point of the soliton length. As higher-order solitons are intrinsically unstable in the presence of higher-order dispersion and Raman gain, in reality they do not usually oscillate over several cycles. Therefore, the length of fiber used must be significantly less than the soliton length. Compression of this type in HC-PCF was first demonstrated by Ouzounov *et al* [12], who compressed a 120fs pulse to 50fs in 0.24m fiber. An empirical limit for this compression was proposed by Dianov *et al* [13] as $\tau_{FWHM}/\tau_{min}=4.1N$. A disadvantage of soliton effect compression is that the compression is never perfect – there is always some radiation which is not compressed, and continues to disperse.

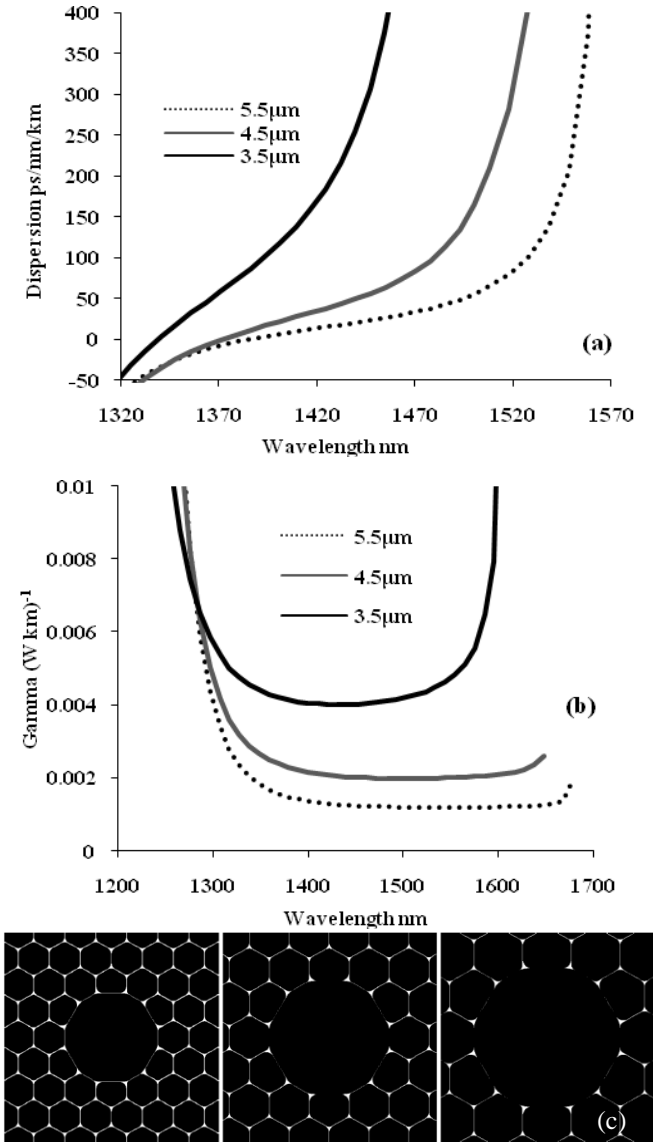


Fig. 1. The modeled dispersion (a) and nonlinearity (b) of 3 different 7-cell fibers designed such that the high frequency edge of their bandgaps occurs at the same wavelength. The pitches of these fibers are 3.5, 4.5 and 5.5 μm (c).

A different means of compressing a pulse is the adiabatic compression of a fundamental soliton. In adiabatic soliton compression the dispersion of the fiber is decreased slowly along its length. The effects of dispersion and SPM must balance for a soliton to remain in its fundamental form; and so a decrease in the value of dispersion results in an increase of bandwidth until SPM and dispersion become rebalanced. Therefore, a slow decrease in dispersion along a waveguide will result in a shorter pulse being created, according to equation (1).

In HC-PCF this decrease in dispersion at a fixed wavelength can be achieved by shifting the bandgap to longer wavelengths through up-tapering the outer diameter of the fiber such that it increases along its length. For this transition to be adiabatic, the change of dispersion must be slow relative to the soliton length. Hence, for a large compression ratio the taper length needs to be many times the soliton length. Of course as the pulse gets temporally shorter the soliton length gets shorter. Therefore, it should be possible to shorten the

taper by having a nonlinear gradient which gets steeper towards the end of the taper where the pulse is shorter. However, Pelusi *et al* [14] suggest that this does not aid in shortening the taper greatly. Theoretically, the main advantage of adiabatic compression over soliton effect compression is that the all the energy of the input pulse is contained in the output pulse. However, due to fiber attenuation, third order dispersion and Raman scattering, this is not usually the case experimentally. It has been shown to be possible to suppress the Raman self frequency shift of a soliton in HC-PCF by filling it with a non-Raman-active gas such as Xenon [12].

Adiabatic compression was first demonstrated in a HC-PCF taper by Gêrôme *et al*. They fabricated an 8m taper compressing 195fs pulses to less than 100fs at 800nm [15].

An obvious consideration is what are the limitations to compression using these techniques? Gorbach and Skryabin [16] state that in terms of pulse length there is a barrier imposed by Raman gain: if the bandwidth of the pulse gets large then it encloses the Raman gain peaks and much of the pulse is transformed into non-solitonic radiation. This will be more problematic in adiabatic compression due to the propagation distances involved. The Raman gain spectrum of air is centered at 2.6THz [17], [18] which is a fifth that of silica at 13THz. Hence, pulses in air with durations less than or close to 100fs suffer from strong losses of energy being coupled to non-solitonic radiation.

Another limitation on the ultimate pulse length is third order dispersion [12]. Hence, the dispersion of the fiber needs to be as flat as possible for optimal compression. This also means that to demonstrate large compression ratios it is better to start with longer picosecond pulses, which is the case investigated here.

III. EXPERIMENTAL RESULTS USING 3-CELL HC-PCF

A. Fiber Parameters

Two 3-cell fibers are presented within this paper. The two fibers had virtually the same cladding structure, but the structure of the core and the cells surrounding the core differed. One had a large (10 μm diameter) core that perturbed the surround structure greatly, and the other had a 6.5 μm diameter core which perturbed the surrounding cladding by far less (Fig. 2). These core geometries were chosen as they suppressed the effects of surface mode anti-crossings near the centre of the bandgap. For comparison, we also show results from one of our state-of-the-art 7-cell fibers which has a core diameter of 16.7 μm [9].

The attenuation and dispersion of the 3-cell fibers was measured and is shown in Fig. 3. The dispersion was measured using a low coherence interferometric technique. The minimum attenuation of both of these fibers is less than that reported by Petrovich *et al* [8] (which was approximately 200dB/km) although the bandwidth is also less in both cases.

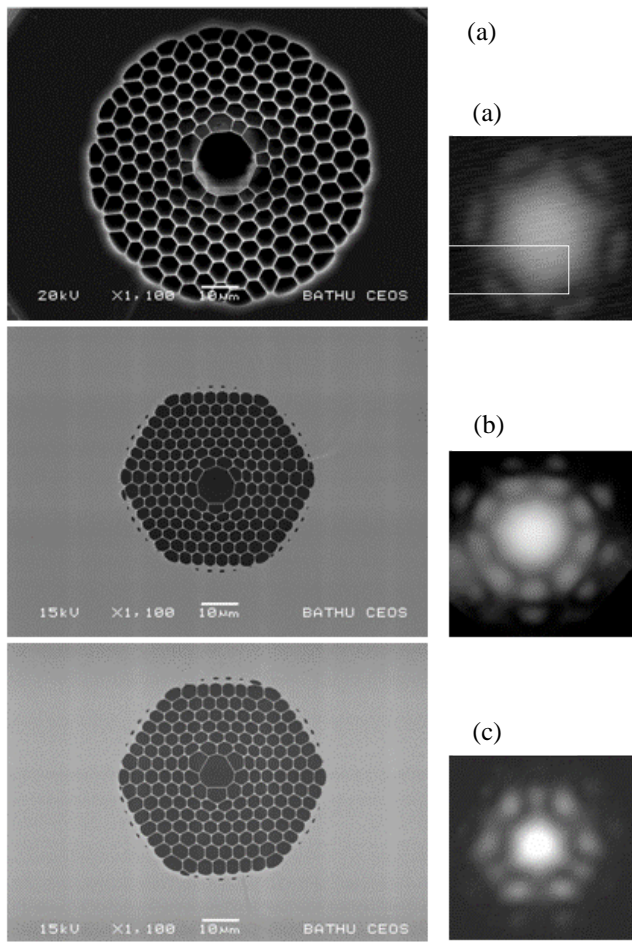


Fig. 2. A Scanning electron micrograph of a state-of-the-art 7-cell fiber (a), and an example modal field pattern measured for a wavelength at the center of the bandgap. Also presented are micrographs and modes for the two 3-cell fibers, with a 10µm core (b) and a 6.5µm core (c).

For both 3-cell fibers, the dispersion and dispersion slope was found to be high across much of the bandgap with the larger 10µm core fiber having a relatively flat region at the centre of the bandgap (Fig. 3a). The increased dispersion in a 3-cell HC-PCF arises due to the stronger confinement in a smaller core compared with the 7-cell fiber (or in fact a 19 cell fiber, which theoretically has even flatter dispersion).

Modeling was done on a 3-cell fiber with the same core geometry as the 6.5µm fiber (Fig. 4), but with slightly different values of pitch, core size and air filling fraction. A 7-cell fiber was also modeled with the same cladding for comparison. The respective core sizes were 10µm and 15µm. The cladding had hexagonal holes with rounded corners; a pitch of $\Lambda=5\mu\text{m}$, a strut thickness of 0.02Λ and a curvature at the corners of 0.41Λ .

The nonlinear coefficient γ and dispersion D was evaluated across the bandgap for both cases (Fig. 5). Comparing the modeled 3-cell fiber and 7-cell fiber the nonlinear coefficient, γ , of the 3-cell is approximately 7 times greater. In the 7-cell fiber, 20% of the Kerr nonlinear response comes from silica. This silica contribution is 25 times greater in the 3-cell fiber. The remaining 80% of the Kerr nonlinear response of the 7-cell fiber comes from air. This air contribution is twice as large in the 3-cell fiber. The dispersion of the 3-cell fiber is

larger by a factor of 4 (10nm from the ZDW). Hence, the soliton energy at this wavelength is only decreased by a factor of approximately 2 between these two designs. These ratios will not hold true for all 3-cell fibers and 7-cell fibers as the properties of HC-PCF differ significantly with changes in pitch and air-filling fraction, for example.

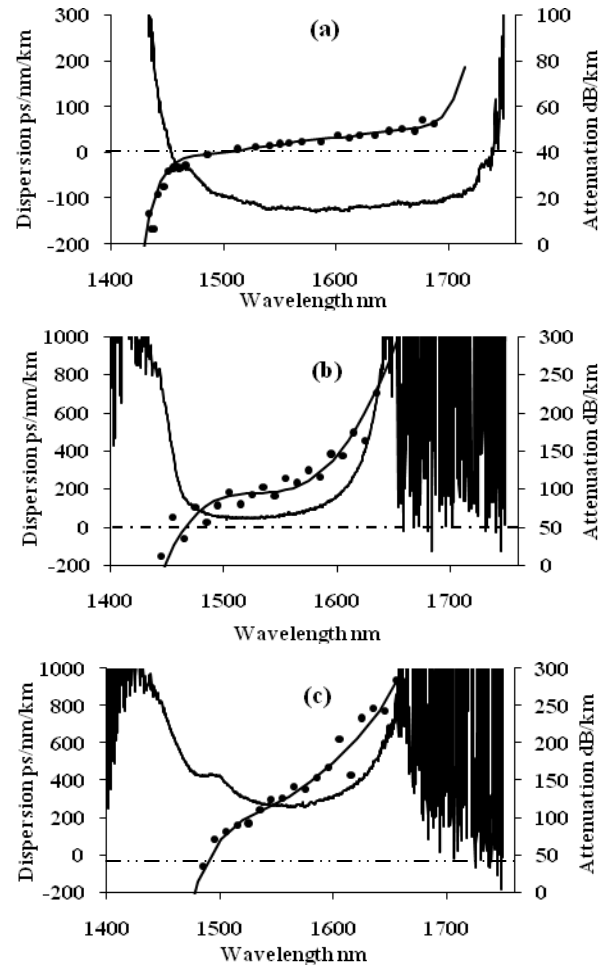


Fig. 3. In (a), the measured attenuation and dispersion of the state of the art 7-cell fiber, (b) the 10µm core fiber and (c) the 6.5µm core fiber. The zero dispersion wavelengths are 1502nm, 1465nm and 1490nm respectively. The dispersion curves were obtained by measuring the group delay as a function of wavelength. The points represent the two-point difference between adjacent measured points and the lines are the differential of a 6th order polynomial fit line.

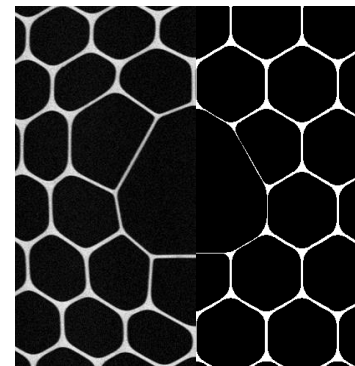


Fig. 4. A comparison of the modeled 3cell fiber structure (right half) to that of the fabricated 6.5µm fiber (left half) the two halves are scaled to fit together; the pitches differ.

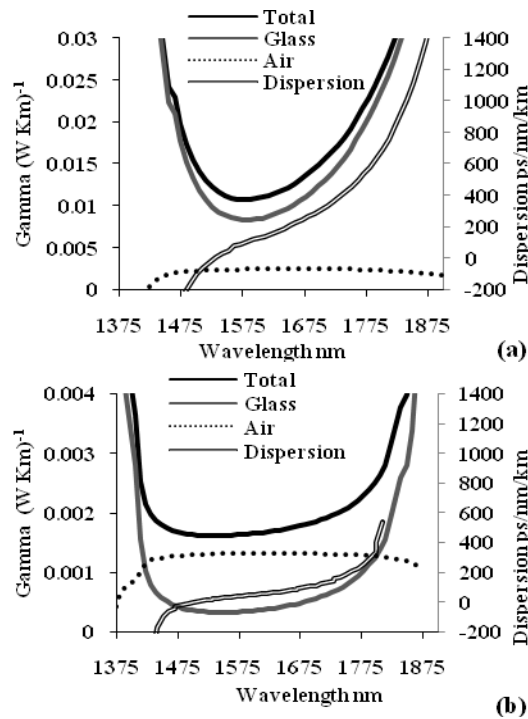


Fig. 5. In (a), the calculated γ and dispersion for the modeled 3-cell fiber in Fig. 4, and (b) the modeled 7-cell.

B. Experiment

For these experiments the laser system used was a femtosecond optical parametric amplifier (OPA). This was pumped by a regeneratively amplified Ti-Sapphire laser system. The amplifier delivered 200fs pulses centered at 802nm and with energies up to 5 μ J at a repetition rate of 125kHz. The OPA allowed the generation of 90fs pulses that could be tuned across the entire bandgap of both 3-cell fibers. The maximum pulse energy obtainable at 1500nm was 275nJ.

For the 10 μ m core diameter 3-cell fiber some spectral splitting was seen for launching the pulse at the ZDW [19], but nothing was observed away from this wavelength. Using an autocorrelator, and the 6.5 μ m core diameter fiber, pulses were observed through the 5m of fiber. Light was launched into the fiber with a maximum coupling efficiency of 30%, well below the 50% coupling efficiency which was typically obtained using the 7-cell fiber. We believe this to be due to the reduced overlap of a Gaussian beam with the guided mode of the 3 cell fiber.

For both 3-cell fibers the position of spectral splitting at their respective ZDW's agreed with the values from the low coherence interferometer measurements. Fig. 6 shows this agreement in ZDW for the 6.5 μ m 3-cell fiber putting it at 1490nm.

C. Results

Launching pulses at 1500nm into the 5m long 6.5 μ m core fiber, a self frequency shift was observed with increasing pulse energy (Fig. 7). Launching 275nJ pulses at the fiber input face (the coupled energy was less due to the estimated 30% coupling efficiency), an output energy of 80nJ was measured and a 435fs pulse was observed on an autocorrelator. This is much shorter than the multi-picosecond

pulse expected for linear propagation given that the dispersion is approximately 100fs/nm/m at 1500nm, and that an output spectral width of 5nm was seen after 5m. The input pulse spectrum was of a similar shape to that in Fig. 6.

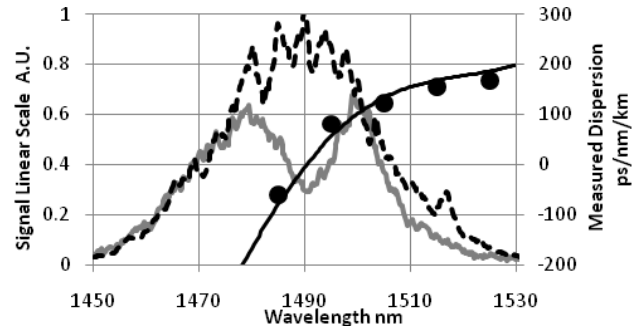


Fig. 6. In grey the spectral splitting observed launching at the 5m fiber an 80nJ input pulse (not the coupled energy) shown in dashed black. Both curves are arbitrary and individually normalized. In black, a part of the measured dispersion taken from Fig. 3c.

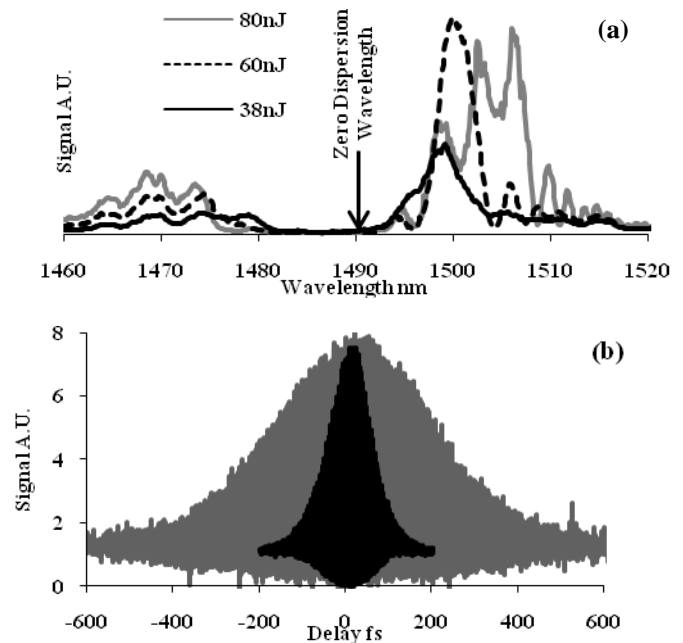


Fig. 7. In (a), the spectral response through 5m of the 6.5 μ m fiber for different output pulse energies and (b), autocorrelations of the input pulse in black (90fs) and the output pulse in grey (435fs), for a measurement of 80nJ at the output.

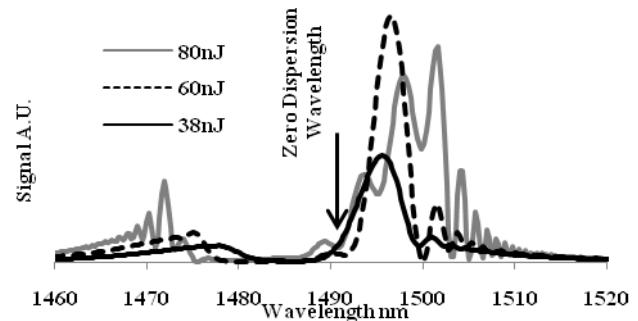


Fig. 8. The modeled spectral response of 5m of 6.5 μ m 3-cell fiber for different input pulse energies. The input pulse was a 90fs sech^2 shaped pulse centered at 1492nm.

In an effort to reproduce the results in Fig. 7a modeling was done using a split step Fourier method, (equation 1 from [16]); fiber losses were not included, a coupling efficiency of 100% was assumed and higher-order dispersion terms were taken from a polynomial fit to data in Fig. 3c. Observing Fig. 5a the relative nonlinear contributions of air and glass were taken to be in a 1:3 ratio, gamma was assumed to be $0.0138 \text{ (W km)}^{-1}$ (slightly higher than the modeled value). Good agreement was found with the experimental results, (Fig. 8). The computed output pulse length was 330fs for the input of a 90fs, 80nJ input pulse.

We conclude that the potential benefit of using the 3-cell design over the 7-cell design for low energy solitons which is associated with the increase in nonlinearity is negated by increased dispersion. The magnitude of the group-velocity dispersion across the bandgap is large because of the dispersion slope. The fabricated 7-cell in Fig. 3 had a dispersion slope at the centre of the bandgap of $0.3\text{fs/nm}^2/\text{m}$ compared to over $2\text{fs/nm}^2/\text{km}$ for the $6.5\mu\text{m}$ 3-cell. The modeled 7-cell and 3-cell fibers have dispersion slopes of $0.2\text{fs/nm}^2/\text{m}$ and $1.6\text{fs/nm}^2/\text{m}$ respectively.

Placing the guiding core of the 3-cell in the centre of the cladding structure rather than off-centre as in our designs would have made the stacking process more difficult, as the outer ring of cladding holes would be less symmetric. However, a central core might have enabled the fabrication of 3-cell fibers with higher air filling fractions giving broader low-loss regions and hence reduced dispersion slope (Fig. 1). The asymmetry of the off-center core makes it harder to increase the air fraction without distorting the fiber structure.

IV. TAPER COMPRESSION

A. Tapered fiber

A tapered HC-PCF was made during the draw of the standard 7-cell HC-PCF shown in Fig. 9. Also shown, is an attenuation measurement of the uniform fiber. It has an attenuation of approximately 125dB/km at 800nm giving the 35m taper an estimated loss of 4dB. This loss sets the limit on the maximum length of the taper, as any loss has to be compensated by a decrease in dispersion, or it will result in an increase in output pulse length (1).

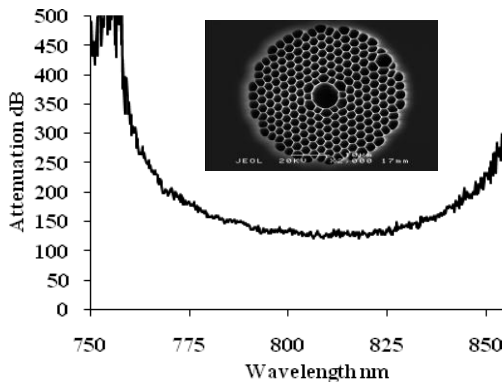


Fig. 9. The attenuation measurement of a fiber with a constant outer diameter created at the same time as the taper, an SEM is inset.

The taper was fabricated by varying the capstan speed during the drawing process. Rather than fabricating a taper with a diameter change over only the desired 35m, a long taper was fabricated and the required 35m length was carefully selected. This was done by measuring the transmission of lengths cut off the ends of the taper, and a measurement was performed on two 0.5m lengths to confirm the dispersion at either end of the taper using a low coherence interferometric technique (Fig. 10). The method is described in detail in [15].

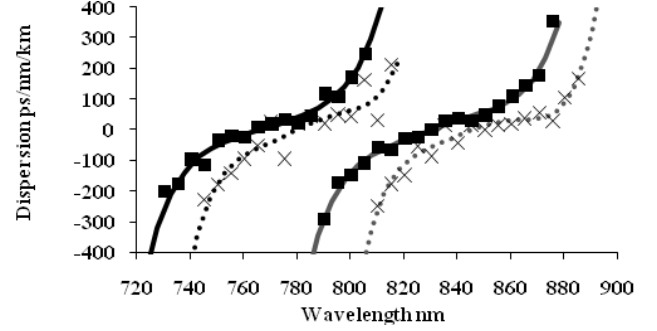


Fig. 10. The measured dispersion of both ends of the taper (black is input, grey is output). The solid and dotted curves correspond to different polarization states; the solid curves correspond to the polarization used in this experiment.

At 802nm wavelength, the dispersion is 150fs/nm/m at the fiber input, and at the output the ZDW is 830nm. The output dispersion was minimized at 830nm rather than 802nm as the effect of the soliton self-frequency shift is to increase the wavelength of the propagating soliton [20], [21].

B. Experiment

The laser system used was a regeneratively amplified mode-locked Ti-Sapphire laser, which gave transform limited 200fs pulses centered at 802nm with a repetition rate of 250KHz and up to 4.4μJ pulse energy. These pulses were then processed using a Fourier plane pulse shaper [22], where the spectral bandwidth was reduced using an adjustable opaque slit placed in the Fourier plane, temporally broadening the pulse. This simple filtering keeps the time bandwidth product small, while losing much of the input power. Two pulse lengths were chosen for the experiments; 1.2 and 2.5ps.

These pulses were coupled to the fiber with an estimated efficiency of 65%, and the polarization was rotated until optimal compression was observed: corresponding to the black dispersion curves in Fig. 10.

C. Results

For both input pulse lengths, the input energy was increased whilst observing the output pulse length until optimal compression was achieved. Fig. 11 shows the spectral and temporal changes for separately launching 80nJ, 1.2ps and 55nJ 2.5ps pulses into the taper. For these 2 different input pulses deconvolved output pulse lengths of 175 and 215fs respectively were recorded on an autocorrelator based on two photon absorption in a LED [23].

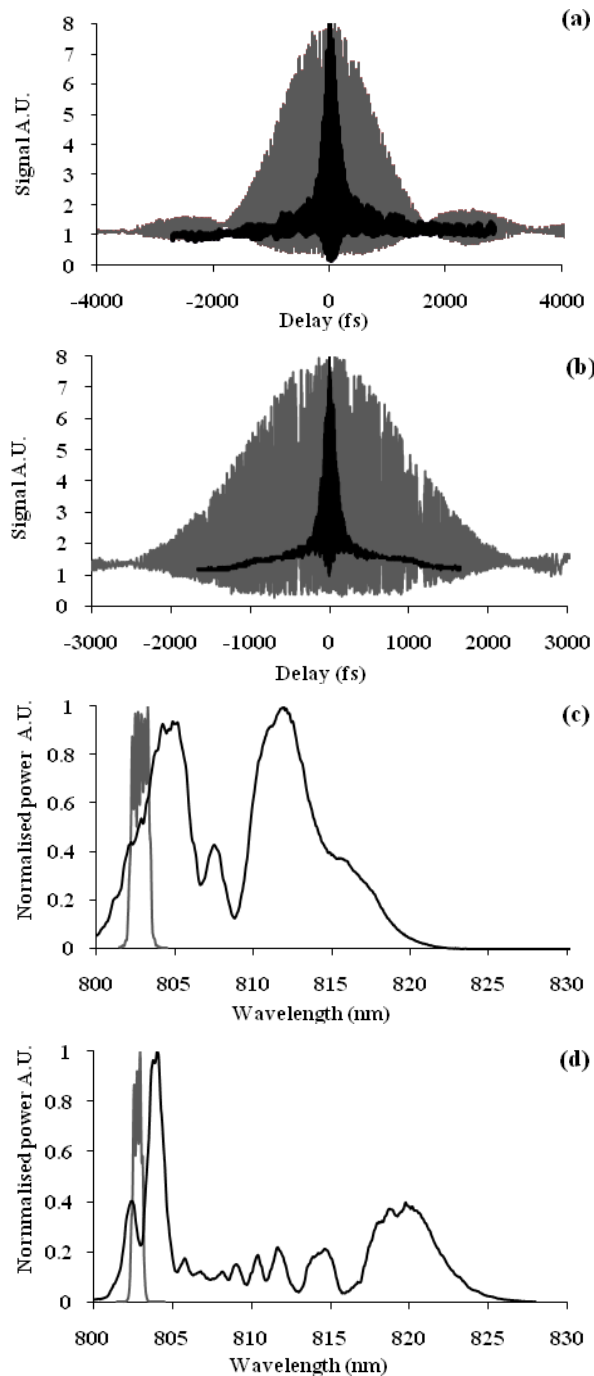


Fig. 11. (a)&(b). Input and output autocorrelations for the 1.2 and 2.5ps input pulses respectively, for output pulse energies of 19.4 and 13nJ. (c)&(d) The respective corresponding spectra for these autocorrelations. For all cases grey is the input pulse and black is the output pulse.

Observing the output pulses on a GRENOUILLE, (Swamp Optics) confirmed the presence of compressed pulses at 812 and 820nm respectively (Fig. 12) hence it is believed that both these spectral peaks correspond to the soliton-effect compressed pulse. The GRENOUILLE computed pulse lengths of 138 and 265fs respectively for these traces. Spectrally from Fig. 11c and Fig. 11d both peaks are broader than the input pulse, both having approximately 4.3nm bandwidth and hence setting a lower bound for the pulse length of 155fs at this wavelength.

The output traces for the 1.2ps pulse from both the GRENOUILLE and the autocorrelator are clean. However for the 2.5ps input pulse it is evident that the output pulse sits on a pedestal, which can be expected from study of the corresponding spectrum. The oscillations in the input pulse spectra, Fig. 11c and Fig. 11d, are an effect of the spectral filtration method used.

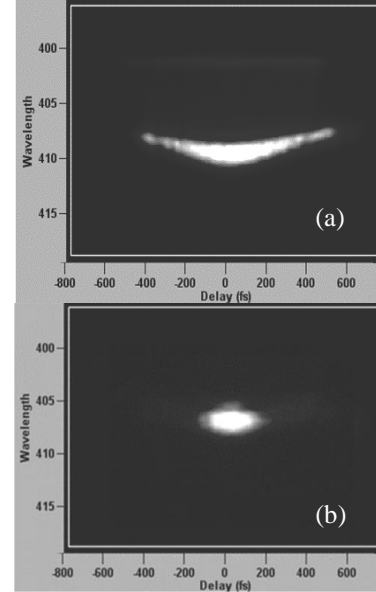


Fig. 12. (a) The output trace on a GRENOUILLE for the 1.2ps input pulse, the calculated pulse length was 138fs. Visible is the spectral peak at 812nm from Fig. 11c. (b) The output trace for the 2.5ps input pulse, the calculated pulse length was 265fs. Visible are the spectral peaks at 804 and 820nm from Fig. 11d. Note: Because the GRENOUILLE uses second harmonic generation to measure pulse lengths, the wavelength scale should be doubled to return real values of wavelength.

The large compression ratios – 7 times and 12 times for the 1.2 and 2.5ps input pulses respectively – in such a short taper are impressive. In the case of the 1.2ps input pulse we estimate based on the spectrum that roughly 50% of the output energy is in the compressed pulse. For this case, the input soliton length is 14m, and this length decreases as the pulse is compressed, therefore we expect adiabatic compression to be significant. For the 2.5ps pulse the input soliton length (60m) is longer than the entire taper, and spectrally it is obvious that less of the input pulse has been converted into the compressed pulse (around 37%). Based on analysis of the spectrum we determine the compressed output energies as 9.4nJ and 5nJ respectively. Assuming a coupling efficiency of 60%, the input pulse energies in the two cases are 47nJ (for the 1.2ps pulses) and 33nJ (for the 2.5ps pulses.) Based on the fiber parameters, this allows us to estimate the input soliton order as $N=2.4$ for the 1.2ps case and $N=2.8$ for the 2.5ps case. As in previous work with conventional [14] and solid-core photonic crystal [24] fibers, optimum compression with short tapers is found to be in the regime of somewhat above the fundamental soliton energy, although the soliton numbers here are slightly higher than in previous work. Table I compares the results from this paper to previously referenced experimental HC-PCF papers in soliton compression.

TABLE I
A comparison of different soliton compression papers in HC-PCF.

Paper	Delivery of sub-100fs pulses through 8m of hollow core fiber using soliton compression F.G��r��me <i>et al</i> [15]	Soliton pulse compression in photonic bandgap fibers D. G. Ouzounov <i>et al</i> [12]	This work; 1.2ps input pulse	This work; 2.5ps input pulse
Compression mechanism	Adiabatic	Soliton effect	Both	Both
Taper	Yes	No	Yes	Yes
Compression Ratio	x2	x2	x7	x12
Fiber length	8m	0.24m	35m	35m
Input soliton length	0.7m	0.6m	14m	60m
Estimated input soliton number	1.6	3.5	2.4	2.8

The dispersion is normal at the output of the taper for the 1.2ps input pulse. When the taper output was cut back by 5m the measured output pulse length increased. This may be due to the difficulty of accurate non-destructive measurement of the dispersion profiles in the rapidly tapered fiber.

V. CONCLUSION

We have demonstrated nonlinear propagation in a 3-cell fiber, where a reduced core area increases the nonlinear coefficient γ . However, this also increases the dispersion, and the overall reduction in soliton energy is just a factor of approximately 2. It may be possible to improve this performance by fabricating fibers with a central hollow core, rather than off-center as in this work. We also demonstrate soliton effect compression in a 35m taper using picosecond input pulses achieving over an order of magnitude temporal compression.

ACKNOWLEDGMENT

The authors acknowledge the help of Alan George and Steve Renshaw in fabricating the fibers. This work was funded by the UK EPSRC, the FP6 project "NextGenPCF", and the FP7 project "CARS Explorer" funded by the European Commission. WJW is a Royal Society University Research Fellow.

REFERENCES

- [1] D. G. Ouzounov et al, "Generation of Megawatt Optical Solitons in Hollow-Core Photonic Band-Gap Fibers," *Science*, vol 301, pp 1702-1704, Sept, 2003.
- [2] F. Luan et al, "Femtosecond soliton pulse delivery at 800nm wavelength in hollow-core photonic bandgap fibers," *Optics Express*, vol 12, pp 835-840, March, 2004.

- [3] A. Hasegawa and F. Tappert, "Transmission of stationary nonlinear optical pulses in dielectric fibers. I. Anomalous dispersion," *Appl. Phys. Lett*, vol 23, pp 142-144, Aug, 1973.
- [4] G.P. Agrawal, *Nonlinear Fiber Optics*, 4th Ed, Academic Press. 2007.
- [5] F. G  r  me, P. Dupriez, J. Clowes, J. C. Knight and W. J. Wadsworth, "High power tunable femtosecond soliton source using hollow-core photonic bandgap fiber, and its use for frequency doubling," *Optics Express*, vol 16, pp 2381-2386, Feb, 2008.
- [6] J. Laegsgaard and P. J. Roberts, "Dispersive pulse compression in hollow-core photonic bandgap fibers," *Optics Express*, vol 16, pp 9628-9644, June, 2008.
- [7] C. J. S. de Matos et al, "All-fiber format compression of frequency chirped pulses in air-guiding photonic crystal fibers," *Phys Rev Letters*, vol 93, Sept, 2004.
- [8] M. N. Petrovich, F. Poletti, A. van Brakel and D. J. Richardson, "Robustly single mode hollow core photonic bandgap fiber," *Optics Express*, vol 16, pp 4337-4346, March, 2008.
- [9] R. Amezcua-Correa et al, "Control of surface modes in low loss hollow-core photonic bandgap fibers," *Optics Express*, vol 16, pp 1142-1149, Jan, 2008.
- [10] R. Amezcua-Correa, N. G. Broderick, M. N. Petrovich, F. Poletti and D. J. Richardson, "Optimizing the usable bandwidth and loss through core design in realistic hollow-core photonic bandgap fibers," *Optics express*, vol 14, pp 7974-7985, Aug, 2006.
- [11] J. L  gsgaard, A.N. Mortensen and A. Bj  rklev, "Mode areas and field-energy distribution in honeycomb photonic bandgap fibers," *J. Opt. Soc. Amer. B*, vol 20, pp 2037-2045, Oct, 2003.
- [12] D. G. Ouzounov et al, "Soliton pulse compression in photonic band-gap fibers," *Optics Express*, vol 13, pp 6153-6159, Aug, 2005.
- [13] E. M. Dianov, Z. S. Nikonova, A. M. Prokhorov, and V. N. Serkin, "Optimal compression of multisoliton pulses," *Sov. Tech. Phys. Lett.*, vol. 12, pp. 311-313, 1986.
- [14] M. D. Pelusi and Hai-Feng Liu, "Higher Order Solitons Pulse Compression in Dispersion-Decreasing Optical Fibers," *IEEE J. Quantum Electron*, vol 33, Aug, 1997.
- [15] F. G  r  me, K. Cook, A. K. George, W. J. Wadsworth and J. C. Knight, "Delivery of sub-100fs pulses through 8m of hollow-core fiber using soliton compression," *Optics Express*, vol 15, pp 7126-7131, May, 2007.
- [16] A.V. Gorbach and D. V. Skryabin, "Soliton self-frequency shift, non-solitonic radiation and self-induced transparency in air-core fibers," *Optics Express*, vol 16, pp 4858-4865, March, 2008.
- [17] M. Mlejnek, E. M. Wright and J. V. Moloney, "Dynamic spatial replenishment of femtosecond pulses propagating in air," *Optics Letters*, vol 23, pp 382-384, March, 1998.
- [18] E. T. J. Nibbering, "Determination of the inertial contribution to the nonlinear refractive index of air, N₂, and O₂ by use of unfocused high-intensity femtosecond laser pulses," *J. Opt. Soc. Amer. B*, vol 14, pp 650-660, March, 1997.
- [19] V. P. Yanovsky and F. W. Wise, "Nonlinear propagation of high-power, sub-100fs pulses near the zero-dispersion wavelength of an optical fiber," *Optics Letters*, vol 19, pp 1547-1549, Oct, 1994.
- [20] J. P. Gordon, "Theory of the soliton self-frequency shift," *Optics Letters*, vol 11, pp. 662-664, Oct, 1986.
- [21] F. M. Mitschke and L. F. Mollemauner, "Discovery of the soliton self frequency shift," *Optics Letters*, vol 11, pp 659-661, Oct, 1986.
- [22] A. M. Weiner, J. P. Heritage and E. M. Kirschner, "High-resolution femtosecond pulse shaping," *J. Opt. Soc. Amer. B*, vol 5, pp 1563-1572, Aug, 1988.
- [23] D. T. Reid, M. Padgett, C. McGowan, W. E. Sleat and W. Sibbett, "Light-emitting diodes as measurement devices for femtosecond laser pulses," *Optics Letters*, vol 22, pp 233-234, Feb, 1997.
- [24] J. C. Travers et al, "Optical pulse compression in dispersion decreasing photonic crystal fiber," *Optics Express*, vol 15, pp 13203-13211, Sept, 2007.



Matthew G. Welch was born in Bradford, Yorkshire, UK in 1984. He received a M.Phys. degree in physics from the University of Bath, Bath, UK in 2006

He is currently studying for a Ph.D. at the University of Bath. He is interested in the propagation of femtosecond pulses in hollow core photonic crystal fiber.